Received: 10 April 2020 | Accepted: 20 May 2020

DOI: 10.1111/gcb.15207

PRIMARY RESEARCH ARTICLE

Global Change Biology WILEY

Agricultural acceleration of soil carbonate weathering

John H. Kim[1] | Esteban G. Jobbágy[2] | Daniel D. Richter[3] | Susan E. Trumbore[1] | Robert B. Jackson[4]

[1]Max Planck Institute for Biogeochemistry, Jena, Germany

[2]Grupo de Estudios Ambientales, IMASL, Universidad Nacional de San Luis/CONICET, San Luis, Argentina

[3]Nicholas School of the Environment, Duke University, Durham, NC, USA

[4]School of Earth, Energy, and Environmental Sciences, Stanford University, Stanford, CA, USA

Correspondence
John H. Kim, Max Planck Institute for Biogeochemistry, Hans-Knöll-Strasse 10, Jena 07745, Germany.
Email: jhk11@duke.edu

Funding information
National Science Foundation, Grant/Award Number: DDIG #0910294, DEB #0717191, GRFP #2006044266 and IOS #0920355; FP7 People: Marie-Curie Actions, Grant/Award Number: FP7-PEOPLE-2013-IEF-626334

Abstract

Soil carbonates (i.e., soil inorganic carbon or SIC) represent more than a quarter of the terrestrial carbon pool and are often considered to be relatively stable, with fluxes significant only on geologic timescales. However, given the importance of climatic water balance on SIC accumulation, we tested the hypothesis that increased soil water storage and transport resulting from cultivation may enhance dissolution of SIC, altering their local stock at decadal timescales. We compared SIC storage to 7.3 m depth in eight sites, each having paired plots of native vegetation and rain-fed croplands, and half the sites having additional irrigated cropland plots. Rain-fed and irrigated croplands had 328 and 730 Mg C/ha less SIC storage, respectively, compared to their native vegetation (grassland or woodland) pairs, and irrigated croplands had 402 Mg C/ha less than their rain-fed pairs ($p < .0001$). SIC contents were negatively correlated with estimated groundwater recharge, suggesting that dissolution and leaching may be responsible for SIC losses observed. Under croplands, the remaining SIC had more modern radiocarbon and a $\delta^{13}C$ composition that was closer to crop inputs than under native vegetation, suggesting that cultivation has led to faster turnover and incorporation of recent crop carbon into the SIC pool ($p < .0001$). The losses occurred just 30–100 years after land-use changes, indicating SIC stocks that were stable for millennia can rapidly adjust to increased soil water flows. Large SIC losses (194–242 Mg C/ha) also occurred below 4.9 m deep under irrigated croplands, with SIC losses lagging behind the downward-advancing wetting front by ~30 years, suggesting that even deep SIC were affected. These observations suggest that the vertical distribution of SIC in dry ecosystems is dynamic on decadal timescales, highlighting its potential role as a carbon sink or source to be examined in the context of land use and climate change.

KEYWORDS

^{14}C, carbon sequestration, climate engineering, crop cultivation, deep drainage, dryland, precipitation gradient, soil inorganic carbon stock

S.E. Trumbore and R.B. Jackson should be considered joint senior author.

1 | INTRODUCTION

Carbon sequestration by storage of organic material in plants and soils is an active policy mechanism to mitigate rising atmospheric CO_2, the key driver of climate change (Intergovernmental Panel on Climate Change [IPCC], 2014). Although the global pool of soil inorganic carbonate (SIC) is comparable in size to the carbon pool in the terrestrial biomass, and carbonate weathering is one of the dominant drivers of atmospheric CO_2 levels on geologic timescales, SIC has received substantially less attention by scientists and policymakers (Jobbágy & Jackson, 2000; Schimel et al., 1995; Schlesinger, 1982). This lack of attention may partly stem from the relatively slow formation rates of SIC (Berner, 2003; Goddéris & Brantley, 2013; Liu & Dreybrodt, 2014), even though the long residence time can be a desirable quality for carbon sequestration (Berner, Lasaga, & Garrels, 1983; Lal & Kimble, 2000; Williams, Walter, Ku, Kling, & Zak, 2003).

Pedogenic carbonates form in chemical weathering reactions involving water, CO_2, and a cation, expressed as (Birkeland, 1999):

$$\begin{aligned} 2CO_2 + 2H_2O &\rightleftharpoons 2H^+ + 2HCO_3^- \\ Ca^{2+} + 2HCO_3^- &\rightleftharpoons CaCO_3 + H_2O + CO_2. \end{aligned} \quad (1)$$

Dissolution of CO_2 in water produces bicarbonate ions (HCO_3^-), which can react with Ca^{2+} or Mg^{2+} to precipitate into solid carbonates, releasing water and CO_2. Additions of CO_2, water, and/or acids thus can push the equilibrium toward dissolution of carbonates. For example, depth to caliche is often positively correlated with depth of rainwater infiltration (Arkley, 1963; Jenny & Leonard, 1934). Once dissolved, bicarbonate may be susceptible to downward leaching under high soil water fluxes or to CO_2 degassing in the presence of acids. For these reasons, pedogenic carbonate formation is more stable under arid and semi-arid climates, with Ca supply limiting precipitation rates and the Ca source (e.g., calcareous or siliceous dust or parent material) determining whether carbonate formation results in carbon sequestration (Schlesinger, 2017).

Some recent studies have hinted at a more dynamic SIC pool in dry ecosystems than previously acknowledged (Liu, Li, & Wang, 2011; Tamir et al., 2011). A study estimated that the carbon sink associated with the carbonate weathering process is comparable to that of the global forest biomass (Liu & Dreybrodt, 2014), and other studies have reported SIC sequestration to be in excess of 0.02 Mg C ha^{-1} $year^{-1}$ under natural vegetation and up to 0.4 Mg C ha^{-1} $year^{-1}$ in managed lands (Bughio et al., 2015; Landi, Mermut, & Anderson, 2003).

The current literature offers more than one hundred comparisons of SIC under natural vegetation and croplands with nearly an even split of comparisons reporting higher SIC with agricultural conversions and vice versa (60 vs. 54 cases, respectively; Appendix S1: Literature synthesis). The majority of these studies focused on the surface soil (sampling depth of <2.5 m with median depth of 0.75 m). Studies that observed decreases in SIC with agricultural conversion have hypothesized erosion and dissolution as responsible mechanisms (e.g., Kalbitz et al., 2013; Papiernik et al., 2007). Studies reporting increases in SIC have generally attributed them to carbonate precipitation triggered by the addition of Ca-rich irrigation waters or by enhanced freeze–thaw cycles (e.g., Bughio et al., 2015; Yu et al., 2014). Analyses of national soil inventories and a recent meta-analysis have similarly found little-to-mixed evidence of land-use effect on SIC while also noting shallow sampling depths of many studies and inventories (An, Wu, Zhang, & Tang, 2019; Berhongaray, Alvarez, De Paepe, Caride, & Cantet, 2013; Wu, Guo, Gao, & Peng, 2009). Lack of consensus and limited sampling depths seem to impede conclusions on the net effects of cultivation on SIC (Figure S1).

Our goal was to compare deep SIC storage and dynamics based on carbon isotopes under paired land uses to see whether this supposedly stable pool of carbon may respond to land-use-induced changes in soil water fluxes at decadal timescales, potentially forcing soils across the threshold between net carbonate accumulation and loss (Chadwick & Chorover, 2001). In this framework, anthropogenic activities such as farming act as a sixth state factor dictating soil formation (Kuzyakov & Zamanian, 2019; Richter Jr., 2007). Water flux and acid–base reactions are primary determinants of whether weathering products (in our case, dissolved carbonate) are retained or flushed (Equation 1). We hypothesized that increased deep drainage and acidification accompanying agricultural conversion of natural vegetation dissolve carbonates (Kim & Jackson, 2012; Moody & Aitken, 1997). If deep drainage is the only important change, transport of dissolved carbonate to groundwater would prevail, whereas if acidification is the dominant change, release as CO_2 would prevail. Although a negative relationship between rainfall and SIC storage across space is well established (Kelly, Amundson, Marino, & DeNiro, 1991; St. Arnaud, 1979), to our knowledge no studies have tested the temporal effect of increased soil water storage and transport on SIC based on the conversion of natural vegetation to croplands.

To examine whether decades-old (30–100 years) cultivation of natural dry ecosystems results in SIC losses, we collected soil samples to 8.5 m depth in eight sites with adjacent or nearby natural vegetation and rain-fed cropland plots, with four of the sites having in addition irrigated cropland plots. We hypothesized that (a) SIC present under natural vegetation will experience net losses under cultivation that will be proportional to increases in storage and transport of soil water and these losses would be larger under irrigated conditions, (b) given accelerated weathering and equilibration in wetter conditions (Amundson et al., 1994; Gocke, Pustovoytov, & Kuzyakov, 2010; Van Breemen & Protz, 1988), SIC under croplands will reflect modern crop inputs compared to the more stable SIC pools under natural vegetation. Specifically, we expected SIC under croplands to have higher percent modern carbon (pMC) and to reflect exchange with crop-respired CO_2 in its $\delta^{13}C$ compared to those of SIC under natural vegetation.

2 | METHODS

2.1 | Site description and soil sampling

We selected five sites in the southern Great Plains of the United States and three sites in the Pampas grasslands of Argentina along a

precipitation gradient (400–900 mm/year) to examine potential interactions between land-use change and climate for altering ecosystem storage of SIC (Kim & Jackson, 2012; Kim, Jobbágy, & Jackson, 2016; see Figure S2 map of our sites). Arid and semi-arid regions, including our study areas, contain virtually all of the terrestrial SIC (Lal & Kimble, 2000) and have also experienced widespread conversion to crop cultivation (Ramankutty, Evan, Monfreda, & Foley, 2008), providing a relevant and representative setting to test the effects of land-use change on SIC storage. Rain-fed and, where available, irrigated cropland plots were paired with an adjacent or nearby natural vegetation plot (<1 km away; Table 1). All plots were greater than 2.5 ha in size, and the cropland plots had been under the current land uses for 30–100 years. The sites were located on loess or calcareous deposits (Table 1). Soil maps were consulted prior to site selection to ensure that the land-use plots were on the same soils at our sites (United States Department of Agriculture [USDA] Soil Survey Staff, 2009). We also surveyed landowners and farm managers for land-use history at each site, including cropping schemes (e.g., species, rotations) and inputs (e.g., fertilizers, pesticides, and irrigation; Table 1). Most cropland plots were also limed every few years to counter agricultural soil acidification, which typically results from an imbalance in the nitrogen cycle from fertilization, removal of base cations through harvest, or greater biological activities (Moody & Aitken, 1997). Mean annual precipitation was calculated from long-term (>40 years) records maintained by weather stations within 30 km of the sites (Instituto Nacional de Tecnología Agropecuaria [INTA], 2010; National Oceanic and Atmospheric Administration [NOAA],

TABLE 1 Site information. San Angelo, Goodwell, Quanah, Tribune, and Riesel sites are in the US and Parera, General Levalle and Rio Bamba sites are in Argentina

Site	Lat., long. (°)	Precip., MAT	PWE	Soil and parent material[a]	Dominant species[b]			Land-use age[d]
					Natural vegetation	Rain-fed cultivation[c]	Irrigated cultivation[c]	
San Angelo	31.4, −100.4	514, 18.3	−1,161	Aridic Calciustolls; Angelo clay loam; Calcareous alluvium on Sandstone	*Bouteloua* and *Buchloe* spp. (mix)	Ct (35)	Ct (140)	100, 40
Goodwell	36.6, −101.6	407, 13.4	−1,094	Aridic Paleustolls; Gruver clay loam; Loess on Sandstone	*Bouteloua* and *Andropogon* spp. (C4)	W, So (60)	C, W, So, Su (110)	60, 60
Quanah	34.3, −99.8	679, 16.4	−928	Argiustolls; Sagerton clay loam; Calcareous alluvium on Mudstone	*Stipa* spp. (mix)	W (0)	Ct (110)	100, 60
Tribune	38.5, −101.6	479, 10.5	−830	Aridic Argiustolls; Richfield silt loam; Loess on Sandstone	*Bouteloua* and *Andropogon* spp. (C4)	W (15)	C, So (170)	30, 50
Riesel	31.5, −96.9	890, 19.3	−597	Udic Haplusterts; Heiden clay; Mudstone	*Schizachyrium scoparium* (C4)	C, O, W, P (55)	NA	>100
Parera	−35.1, −64.5	682, 16.3	−503	Entic Haplustolls, Silt loam; Loess on siliciclastic sedimentary rocks	*Prosopis caldenada*, *Stipa* spp. (C3)	C, S, Su, W (30)	NA	90
General Levalle	−34.0, −63.8	889, 16.8	−326	Udorthentic Haplustolls, Loam; Loess on siliciclastic sedimentary rocks	*Distichlis* spp., *Paspalum* spp., *Elymus* spp. (mix)	C, S, Su, W (11)	NA	30
Rio Bamba	−34.1, −63.7	889, 16.8	−326	Udorthentic Haplustolls, Sandy loam; Loess on siliciclastic sedimentary rocks	*Cortadeira selloana* (mix)	C, Su, W (NA)	NA	NA

Abbreviations: MAT, mean annual temperature (°C); Precip., mean annual precipitation (mm/year); PWE, potential water excess (precipitation − potential evapotranspiration, mm/year).

[a]Parent material information from USDA Web Soil Survey and USGS Mineral Resources Online. Argentina sites from Zárate and Tripaldi (2012).

[b]C3, C4, mix: native plant communities predominantly using C3, C4, or a mix of the two photosynthetic pathways, respectively, based on $\delta^{13}C$ of SOC, C-corn (C4), W-wheat (C3), Su-sunflower (C3), So-sorghum (C4), Ct-cotton (C3), O-Oats (C3), P-Peas (C3), S-soybean (C3).

[c]Nitrogen fertilization rate in kg N ha^{-1} $year^{-1}$ averaged over 3–30 years in parentheses.

[d]Years since land-use change. Rain-fed and irrigated cultivation, respectively.

National Climatic Data Center, 2011). Most of our sites were located in agricultural research extension centers with good local records of the weather and land management history.

We took five to eight cores per land-use plot down to 8.5 m depth using a direct-push coring rig (Geoprobe Systems; Jackson, Banner, Jobbágy, Pockman, & Wall, 2002) in the US sites and hand augers at the Argentinean sites. Sampling increments were every 0.3 m in the top 0.61 m of the soil and every 0.61 m thereafter in the US sites, and every 0.2 m to 1 m depth, then every 0.3 m to 4 m depth, and every 0.5 m thereafter in the Argentina sites. The only plots at which soil samples were not retrieved to our full sampling depth was at a grassland plot near San Angelo, TX, where indurated caliche around 5 m depth made deeper coring impossible with our equipment, and Quanah, TX and two sites in Cordoba, Argentina (General Levalle and Riobamba) where water tables at ~7.5 and ~2 m depths, respectively, restricted deeper sample recovery (Table 1). Soil cores were weighed in the field and subsampled into intact core sections for soil moisture. The rest of the cores were sieved, homogenized, and subsampled for elemental analysis and shipped to the laboratory for analysis. Segregated carbonate nodules were recovered from sieving (2 mm mesh) and analyzed separately for SIC content (see below). Samples were collected before crop plantings occurred (February–March in the USA and November–December in Argentina).

One limitation of the space-for-time substitution approach is the unknown initial conditions prior to the land-use changes. Our adjacent or nearby paired land-use plots were located on similar topographic setting and soil (Table 1). To further test whether the plots shared similar geomorphic history, we examined stable carbon isotope ratios ($\delta^{13}C$) in nodular concretions of SIC. Nodular SIC data provide a good test of our plot selection as they represent records of paleoclimate and geomorphic processes but are less vulnerable to short-term land-use changes than diffuse SIC (Zamanian, Pustovoytov, & Kuzyakov, 2016). $\delta^{13}C$ of nodular SIC were not significantly different to $p > .1$ between land uses (Student's t test; Figure S3), indicating that processes governing the formation of these segregated SIC nodules such as soil formation and deposition, carbon inputs, climate, and drainage on geologic timescale were likely consistent between our land-use plots. In addition, radiocarbon values show overall more modern SIC in croplands compared to natural vegetation pairs (see Section 3), a trend opposite to that expected from agricultural topsoil erosion or liming. This evidence suggests our data are likely capturing SIC dynamics associated with enhanced agricultural drainage and acidification rather than other processes associated with cultivation practices or artefacts of site selection.

2.2 | Laboratory analysis

Soil samples were analyzed for soil moisture, bulk density, SIC content, carbonate nodule mass, carbon isotopes for SIC, and anions. Intact soil core sections were oven-dried at 104°C for estimating gravimetric moisture content and at 60°C for homogenized samples for carbon measurement with a Carlo Erba Elemental Analyzer using the two-temperature combustion method (Chichester & Chaison, 1992). Soil texture was determined at 0.15, 0.9, 3.4, and 6.4 m depths for the US sites and at 0.4, 1, 2.5, 4, 6, 8 m depths for the Argentina sites by the pipette method (Klute, 1986) and ranged from loam to clay for the different sites (Table 1). Soil bulk density was calculated from volumes of the soil cores and their estimated dry weights based on gravimetric water contents and field weights. SIC contents are expressed as %C by weight; we note that this differs from carbonate contents reported by local soil surveys, which are $\%CaCO_3$ by weight (United States Department of Agriculture [USDA] Soil Survey Staff, 2009). Inorganic carbon contents (%C) of the soil and carbonate nodules by depth were multiplied by soil and nodule weights and summed to estimate SIC storage. Soil moisture storage was calculated using gravimetric moisture content and bulk density. For anion analysis, sieved, homogenized, and dried soil samples were shaken with equal weights of double deionized water for 4 hr. The mixture was then centrifuged, the supernatant filtered, and the filtrate analyzed for alkalinity by acid titration (American Public Health Association [APHA], American Water Works Association [AWWA], & Water Pollution Control Federation [WPCF], 1992). We note that soil drying tends to reprecipitate dissolved inorganic carbon (DIC) into solid-phase carbonates. Our alkalinity analysis indicates that DIC is a minor component of SIC: SIC contents were typically 1%–7%, whereas DIC contents were 0.001%–0.02% C by mass.

2.2.1 | ^{13}C analyses of SIC

Stable carbon isotope ratios of SIC ($\delta^{13}C_{SIC}$) were analyzed on an isotope ratio mass spectrometer (IRMS) coupled to a Gasbench II (Finnigan MAT DeltaPlus XL) and a CTC PAL-80 autosampler. Soil samples were transferred to 12 ml screw capped Labco exetainer vials with butyl rubber septa, which were pre-flushed with N_2 in a glove box (Assayag, Rivé, Ader, Jézéquel, & Agrinier, 2006). We determined sample weights (0.1–250 mg) from SIC contents to produce approximately 1,500 ppm of CO_2 from acidification of SIC. 1.5 ml of water and 0.5 ml of 85% H_3PO_4 were added to acidify the samples. Vials were shaken and left to equilibrate for 24 hr. Stable carbon isotope ratios are reported as $^{13}C/^{12}C$ ratios in per mil (‰) relative to the international reference material Vienna Pee Dee Belemnite:

$$\delta^{13}C = \left(^{13}C/^{12}C_{sample}\right) / \left(^{13}C/^{12}C_{reference}\right) \times 1{,}000. \quad (2)$$

To verify whether agricultural conversion resulted in incorporation of CO_2 from crops into SIC, we examined whether $\delta^{13}C_{SIC}$ values shifted toward $\delta^{13}C$ of carbonates expected from precipitation of crop-respired CO_2. This comparison was made possible by shifts between C3- and C4-dominated communities in transitions from natural vegetation to croplands (Table 1). To estimate $\delta^{13}C$ of carbonates formed with crop-respired CO_2, we used the following equation:

$$\delta^{13}C_{SIC,crop} = \delta^{13}C_{POM,crop} + (\delta^{13}C_{SIC,N} - \delta^{13}C_{SOM,N}), \quad (3)$$

where $\delta^{13}C_{SIC,crop}$ is $\delta^{13}C$ of carbonates precipitated exclusively from crop-respired CO_2, $\delta^{13}C_{POM,crop}$ is the $\delta^{13}C$ of crop residue or light-fraction

soil organic matter (SOM; density fractionation procedure following Sohi et al., 2001) under croplands, and $\delta^{13}C_{SIC,N}$ and $\delta^{13}C_{SOM,N}$ are the average $\delta^{13}C_{SIC}$ and $\delta^{13}C_{SOM}$ under natural vegetation, respectively). The difference between $\delta^{13}C_{SIC,N}$ and $\delta^{13}C_{SOM,N}$ represents $\delta^{13}C$ enrichment between soil CO_2 and carbonates. The enrichment ranged 12‰–17‰ at our sites, close to 14‰–17‰ enrichment given by others (e.g., Cerling, Quade, Wang, & Bowman, 1989). The shallowest soil layers (0–0.3 m for the US sites and 0–0.2 m for the Argentina sites) were used for measurements of $\delta^{13}C_{SIC,crop}$, $\delta^{13}C_{POM,crop}$, $\delta^{13}C_{SIC,N}$, and $\delta^{13}C_{SOM,N}$.

2.2.2 | ^{14}C analyses of SIC

Radiocarbon concentrations of SIC were measured by accelerator mass spectrometry at the Jena ^{14}C facilities (Steinhof, 2014). Because ^{14}C measurements are costly, we chose the cropland pair with the larger SIC loss (always irrigated plots where available) for comparison with $^{14}C_{SIC}$ under natural vegetation. We further selected a subset of the depths, resulting in about a quarter of all samples selected for ^{14}C analysis. We were unable to analyze samples with low SIC content, and sites where low SIC content hindered full comparison of ^{14}C values under different land uses were excluded from analysis.

Samples were prepared in a similar fashion to that of the aforementioned $\delta^{13}C$ analysis, except for using larger sample quantities (7–800 mg) to yield about 0.8 mg of C as CO_2 and caps with Teflon/silicone septa and additionally underlain Black Viton septa (Sigma Aldrich; Gao et al., 2014). The sample was shaken gently and left to equilibrate at room temperature for at least 24 hr. After preparation, CO_2 was directly extracted cryogenically from the vial headspace into a customized high vacuum extraction line using a 1:1 ethanol–dry ice mix as a water trap and liquid nitrogen for freezing out the CO_2. All radiocarbon values are reported in pMC, which is defined as the fractionation corrected $^{14}C/^{12}C$ ratio (R) between the ^{14}C activity of the sample compared to the new oxalic acid standard (C_{OX}; NBS SRM 4990C) according to Steinhof (2013) and Steinhof, Altenburg, and Machts (2017):

$$\mathrm{pMC} = \frac{R}{0.7459}\frac{1+\delta^{13}C_{OX}}{1+\delta^{13}C}. \quad (4)$$

2.3 | Groundwater recharge estimations

To examine the potential role of deep drainage on SIC storage, we looked for relationships between average SIC contents from individual boreholes and groundwater recharge rates previously reported in Kim and Jackson (2012) calculated from chloride mass balance and tracer displacement methods (Allison & Hughes, 1983; Phillips, 1994; Walker, Jolly, & Cook, 1991). In these methods, Cl^- is taken to be a conservative tracer for soil water movement. For the mass balance approach, atmospheric and anthropogenic inputs are equated to Cl^- output from the root zone into the groundwater table. Assuming steady-state conditions, the recharge rate is expressed as follows:

$$Q_{out} = \frac{Q_{in} \times Cl_{in}}{Cl_{out}}, \quad (5)$$

where Q_{out} is the water flux exiting the root zone per ground area per year or recharge rate ($m^3\ m^{-2}\ year^{-1}$ or m/year), Q_{in} is the average rain and irrigation water flux entering the root zone per ground area per year (m/year), Cl_{in} is the average atmospheric and anthropogenic Cl^- input expressed as the concentration in precipitation (g/m^3), and Cl_{out} is the concentration of Cl^- in the soil water exiting the root zone (g/m^3). The approximate root zone was taken to be the top 2.4 m, below which we found a linear relationship between cumulative Cl^- and cumulative soil moisture content, except for cropland plots where we assumed the root zone to be the top 1 m (Phillips, 1994). At the Tribune, Vernon, and Riesel cropland plots, where we did not observe complete leaching of the Cl^- peak formed under natural vegetation, we also used the Cl^- displacement method to estimate recharge rates based on the migration of the original natural vegetation Cl^- and changes in water profiles (Walker et al., 1991). Calculations for the Cl^- tracer displacement method are as follows:

$$Q = \Delta\theta \times \frac{z_1 - z_2}{t_1 - t_2}, \quad (6)$$

where Q is the recharge rate (m/year), z_1 and z_2 are the depths (m) of the Cl^- fronts corresponding to land uses at years t_1 (new, rain-fed cropland) and t_2 (old, natural vegetation), and $\Delta\theta$ is the average change in soil moisture content (g water/g soil) from natural vegetation to cropland of this depth interval (i.e., θ_1–θ_2). Recharge rates were estimated for all sites except two Argentinean sites with saline soils with naturally high Cl^- levels (General Levalle and Rio Bamba).

2.4 | Dissolution of SIC under the new land uses

Soluble salts that are flushed down the soil profile with the wetting front under agricultural conversion (e.g., Cl^-) may take years to reach the water table in semi-arid regions with thick unsaturated zones (Scanlon, Reedy, Stonestrom, Prudic, & Dennehy, 2005). We hypothesized that for the less soluble soil carbonates, there may be an additional lag in their dissolution and mobilization after the initial infiltration of the wetting front. We estimated the time it takes for the observable SIC loss to occur after infiltration of the wetting front under a new land use (i.e., the number of years for the increase in soil moisture at a given layer to produce statistically significant changes in SIC under new land uses) with the following moisture balance:

$$L = \frac{D_{wf} - D_{SIC}}{Q} \times \Delta\theta \times \rho_{BD}, \quad (7)$$

where L is the lag in years between the onset of higher drainage and detectable loss of SIC at a given depth, D_{wf} is the depth of the wetting front (m), defined as the maximum depth at which statistically significant differences in soil moisture between cropland and natural vegetation plots are observed based on soil moisture content from our

replicate cores ($p < .05$; see Section 2.5 below), D_{SIC} is the maximum depth (m) of statistically significant SIC loss (i.e., SIC loss front), $\Delta\theta$ is the average change in gravimetric soil moisture (g water/g soil) from natural vegetation to cropland within the two fronts (D_{wf} and D_{SIC}), ρ_{BD} is soil bulk density (g soil/cm^3), and Q is recharge rate (m/year) under the cropland plots estimated by Equations (5) and (6) as reported in Kim and Jackson (2012). Multiplying L by Q yields the cumulative soil deep drainage necessary for observable SIC loss. The equation assumes that $D_{wf} > D_{SIC}$ and $\Delta\theta > 0$, which was the case for all our sites. Soil moisture can vary with crop type and temporally during crop development. Though such variations would affect our estimation of soil moisture storage and mass balance, they are mainly restricted to the crop root zone (1 m), whereas almost all D_{wf} and D_{SIC} we estimated are below 1 m depth (e.g., Li & Shao, 2015; Wang, Liu, & Zhang, 2009, see Table 3).

We also estimated DIC flux to the ground water underneath croplands using bicarbonate (HCO_3^-) concentrations below the root zone:

$$Q_{DIC} = Q \times DIC, \tag{8}$$

where Q_{DIC} is the downward DIC flux out of the root zone into the groundwater table (Mg C ha^{-1}year^{-1}), Q is the recharge rate (m^3 ha^{-1} year^{-1}), and DIC is the average concentration of bicarbonate-C in soil water extracts (Mg C/m^3 soil water) below the root zone (>2.4 m for natural vegetation and >1 m for cropland).

2.5 | Statistical analysis

To examine whether land-use changes reduced SIC storage by dissolution with increasing deep drainage (i.e., SIC in natural vegetation > rain-fed > irrigated), we used a multinomial test to compare SIC stocks between the rain-fed and irrigated croplands and native vegetation pairs and triplets. Additionally, we used regression analyses between SIC contents and recharge rates from individual boreholes at each site, with log-transformed recharge rates to satisfy homoscedasticity. To test whether irrigation alone can also result in further SIC losses in croplands, we compared the SIC stocks under irrigated versus rain-fed croplands with paired t test.

To determine at which depths SIC losses under cropland plots were significant compared to natural vegetation, we used Student's t tests on data from individual soil samples. To correct for multiple comparisons, we used Benjamini–Hochberg procedure to control the false discovery rate (Benjamini & Hochberg, 1995). Because data from different depths on same cores are not independent, we corrected for our multi-site comparison only. We used the same procedure to compare soil moisture under the different land uses to determine the wetting fronts under croplands. SIC loss fronts (D_{SIC}) and wetting fronts (D_{wf}) for Equation (7) were determined from these tests. In addition, SIC storage at three depth increments (the top 2.4 m, 2.4–4.9 m, and 4.9–7.3 m) were compared between land uses using Student's t test.

To examine how environmental factors affect soil carbonate storage, we analyzed SIC content from individual soil samples in our field data (n = 1,573) with a linear mixed model using the following environmental variables: land use (natural vegetation, rain-fed cropland, irrigated cropland), potential water excess (PWE = mean annual precipitation − potential evapotranspiration [PET]), mean annual temperature (MAT), depth, and sand content as fixed effects and site as a random effect. PET was calculated by the Penman–Monteith equation using high-resolution climate datasets (Allen, Pereira, Raes, & Smith, 1998; New, Lister, Hulme, & Makin, 2002). Because effective moisture (precipitation − evapotranspiration) is a critical determinant of pedogenesis and soil hydrology (Birkeland, 1999; Kim & Jackson, 2012), we used PWE as an aggregated climate variable to represent aridity index. The same mixed model was used for bicarbonate concentrations in soil water extracts to examine whether net acidification occurred under crop cultivation at our sites.

The same mixed model analyses were also performed for percent modern carbon (pMC_{SIC}) and $\delta^{13}C$ of SIC ($\delta^{13}C_{SIC}$) to examine whether land-use changes resulted in incorporation of modern and crop-respired carbon into SIC and how this was affected by the environmental variables. Because we analyzed a subset of our samples for ^{14}C and ^{13}C measurements, land-use designations for these mixed models were natural vegetation versus croplands. For pMC_{SIC} data, we used a generalized linear mixed model as the data were lognormally distributed. We expected $\delta^{13}C_{SIC}$ to be depleted or enriched depending on whether agricultural conversion resulted in shifts to more C3- or C4-dominated communities, respectively, for each site. Most agricultural conversions resulted in shifts to C3 crops, but irrigated cultivation in Tribune and rain-fed cultivation in Parera resulted in more C4-dominated communities and hence more enriched $\delta^{13}C$ carbon inputs. Because of this, we shifted ^{13}C data for these two conversions around the means of $\delta^{13}C_{SIC}$ under the natural vegetation for our statistical analysis. This allowed us to represent the change in $\delta^{13}C_{SIC}$ in the direction toward the shift expected based on new crop carbon inputs, rather than negative and positive for depletion and enrichment, respectively. The modified $\delta^{13}C$ ($\delta^{13}C'_{SIC,Aij}$) for the two croplands was calculated as follows:

$$\delta^{13}C'_{SIC,Aij} = \delta^{13}C_{SIC,Ni} + \left(\delta^{13}C_{SIC,Aij} - \delta^{13}C_{SIC,Ni}\right) \cdot \operatorname{sgn}\left(\delta^{13}C_{SIC,Ni} - \delta^{13}C_{SIC,crop}\right), \tag{9}$$

where $\delta^{13}C_{SIC,Ni}$ is the average $\delta^{13}C$ of SIC at depth i under natural vegetation, $\delta^{13}C_{SIC,Aij}$ is the $\delta^{13}C$ of SIC at depth i under cropland core j, and sng(x) is the sign function that returns −1, 0, or 1 depending on the sign of x. $\delta^{13}C_{SIC,crop}$ is $\delta^{13}C$ of carbonates precipitated exclusively from crop-respired CO_2 from Equation (3).

3 | RESULTS

We observed significantly less SIC storage to 7.3 m depth under cropland plots compared to their native vegetation in all 12 pairs, indicating that a shift from natural vegetation to cropland may result

TABLE 2 Average SIC storage, SOC storage, recharge rates, and soil water bicarbonate concentrations under each land use by depths

Site	Depth (m)	SIC storage (Mg C/ha)[c]			SOC storage (Mg C/ha)[d]			Recharge (mm/year) and HCO_3^- (C mg/L)[e]		
		Nat.	R-f	Irr.	Nat.	R-f	Irr.	Nat.	R-f	Irr.
San Angelo	0–2.4	1,558 (55)	1,624 (117)	1,444 (116)	129	90	107			
	2.4–4.9	1,851[a] (102)	1,338[b] (43)	1,299[b] (52)	38	23	20	0.47	2.18	60
	4.9–7.3	NA	1,314 (51)	1,151 (64)	NA	11	9	(84.1)	(19.6)	(24.7)
	0–7.3	NA	4,277 (355)	3,895 (510)						
Goodwell	0–2.4	350 (109)	451 (96)	313 (96)	88	78	111			
	2.4–4.9	1,103[a] (148)	663[a] (81)	400[b] (27)	33	26	27	0.08	1.14	59.6
	4.9–7.3	1,291 (139)	1,228 (133)	1,097 (96)	35	28	26	(25.6)	(18.1)	(14.7)
	0–7.3	2,745 (501)	2,342 (499)	1,810 (622)						
Quanah	0–2.4	509[a] (92)	186[b] (53)	183[b] (51)	112	78	88			
	2.4–4.9	481 (103)	201 (61)	235 (52)	29	28	27	0.32	6.36	279
	4.9–7.3	614 (188)	613 (93)	372 (64)	22	29	28	(39.6)	(30.9)	(23.9)
	0–7.3	1,605 (490)	1,000 (297)	790 (226)						
Tribune	0–2.4	200 (41)	253 (13)	232 (35)	119	83	97			
	2.4–4.9	735 (125)	536 (58)	437 (48)	68	56	64	0.17	1.41	146
	4.9–7.3	1,616[ab] (200)	1,740[a] (136)	1,375[b] (119)	43	34	43	(19.8)	(17.8)	(19.3)
	0–7.3	2,551 (481)	2,529 (362)	2,044 (346)						
Riesel	0–2.4	609[a] (35)	160[b] (14)	NA	147	91	NA			
	2.4–4.9	391 (14)	320 (30)	NA	22	14	NA	2	9.32	
	4.9–7.3	313[a] (7)	424[b] (39)	NA	21	19	NA	(31.2)	(26.7)	NA
	0–7.3	1,314 (126)	904 (130)	NA						
Parera	0–2.4	475 (95)	255 (84)	NA	117	98	NA			
	2.4–4.9	391[a] (113)	58[b] (24)	NA	25	24	NA	23.8	57.6	
	4.9–7.3	104[a] (29)	10[b] (8)	NA	16	14	NA	(18.3)	(11.2)	NA
	0–7.3	970 (271)	322 (160)	NA						
Gen. Levalle[f]	0–2.4	102[a] (30)	27.4[b] (7)	NA	30	22	NA	NA	NA	NA
	2.4–7.3	NA	NA	NA	NA	NA	NA	NA	NA	NA
Rio Bamba[f]	0–2.4	46.8[a] (2)	30.0[b] (3)	NA	27	18	NA	NA	NA	NA
	2.4–7.3	NA	NA	NA	NA	NA	NA	NA	NA	NA

Note: [a,b]denote significant differences to $p < .05$ between land uses.

Abbreviations: Irr., irrigated cultivation; Nat., natural vegetation; R-f, rain-fed cultivation.

[c]Standard error from replicate cores in parentheses.

[d]SOC stocks from Kim et al. (2016).

[e]Average bicarbonate-C concentrations below the root zone in parentheses (Figure S5). Recharge and bicarbonate-C values were used to calculate DIC fluxes out of the root zone (Equation 8).

[f]No recharge estimates were made for the two humid sites.

in loss of soil carbonates (multinomial test $p < .0001$; Table 2). Rain-fed cultivation resulted in losses of 328 ± 85 (mean ± *SE*) Mg C/ha of SIC on average and 730 ± 80 Mg C/ha of SIC with irrigated cultivation, values that were about an order of magnitude larger than losses of soil organic carbon storage at our sites (average SOC losses: 34 and 20 Mg C/ha for rain-fed and irrigated cultivation, respectively; Table 2). SIC losses were also statistically significant down to 7.3 m deep at some sites, revealing vulnerability of deep SIC to transformations from land surface changes (Figure 1; Tribune and Riesel, $p < .05$, corrected for multiple comparisons). If attributable primarily to the land-use changes, these losses likely occurred in the last 30–100 years. To our knowledge, this is the first evidence of such large, deep, and rapid loss of SIC with land-use changes.

Soil moisture was lower under natural vegetation than their cropland pairs, supporting the hypothesis that hydrological changes may drive SIC losses (Figure 2; Figure S4; Equation 1). Recharge rates and average SIC by borehole at each site were also negatively correlated, indicating that recharge could be an important mechanism governing SIC dynamics, with the higher downward water flux under croplands leading to increased dissolution and leaching

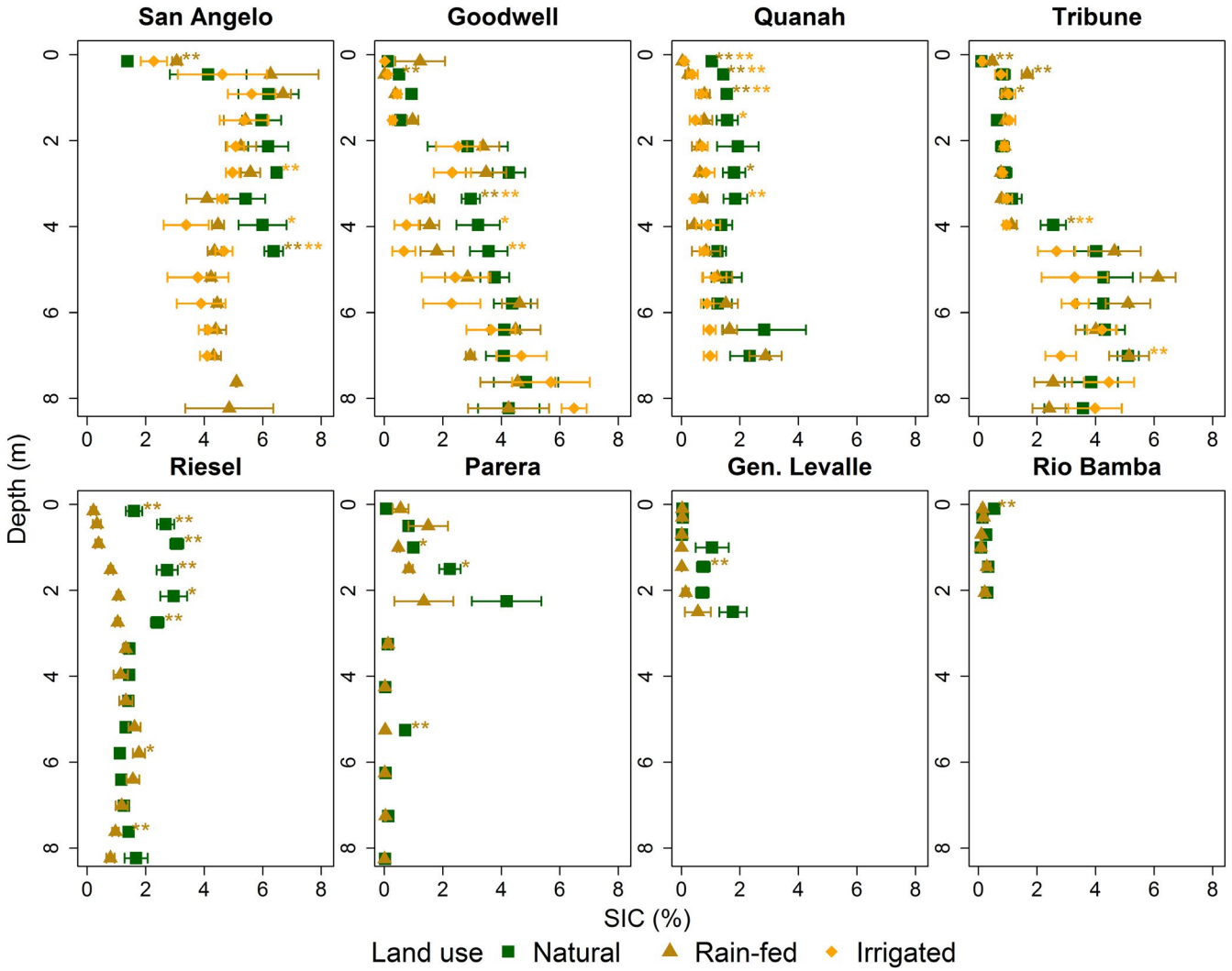

FIGURE 1 Depth profile of soil inorganic carbon (SIC) for the paired land uses by site. Gravimetric SIC content (%C by weight) is presented, including carbonate nodules. * and ** indicate depths with significantly different SIC values between natural and cultivated land uses at $p < .05$, without and with correcting for multiple comparisons, respectively. Sites are ordered from left to right by increasing potential water excess (PWE = precipitation − PET; Table 1). Error bars represent standard error from replicate cores

of native soil carbonates formed or maintained under the drier natural vegetation ($.0001 < p < .037$; average $R^2 = .51$; Figure 2). This possibility is further shown by overall deeper SIC losses (5.3 vs. 2.5 m on average; Table 3) and 402 ± 62 Mg C/ha less SIC stocks under irrigated croplands relative to their rain-fed pairs (paired *t* test $p < .006$; Table 2), where irrigation and the resulting higher deep drainage under otherwise similar land-use practices (e.g., tillage and fertilization) allowed us to isolate the effect of water on SIC (e.g., Magaritz & Amiel, 1981).

SIC losses with land-use changes lagged behind increases in soil moisture, with the depths of SIC loss fronts under cultivation on average located at least 2.5 m above wetting fronts (binomial test $p < .001$; Table 3). At the two sites where our sampling depth captured both of these fronts, there were estimated lags of 26–38 years corresponding to an average cumulative deep drainage of 110 mm, indicating that significant dissolution of native SIC may occur within a few decades of onset of soil wetting from higher recharge (Table 3, Equation 7). Comparatively, the mean age of carbonates under the natural vegetation indicates that SIC was stable for millennia prior to the hydrological changes associated with cultivation (see below for radiocarbon results).

Mixed model analysis found, in order of decreasing importance, depth, PWE, MAT, land use, and sand content to be significant factors affecting average SIC content from individual soil samples (Table S1). SIC decreased with increasing PWE ($p < .0001$), reflecting the fact that arid conditions maintain lower soil water content and deep drainage which tend to accumulate and retain salts and carbonates. Reinforcing the results from the above multinomial test, SIC decreased from natural vegetation to rain-fed and to irrigated croplands ($p < .03$ and .0001, respectively). Together, this evidence indicates that climate, soil, and vegetation factors that enhance deep drainage may increase dissolution of carbonates and decrease SIC storage; additionally, shifting climate patterns may impact the carbon cycle via SIC storage and vice versa.

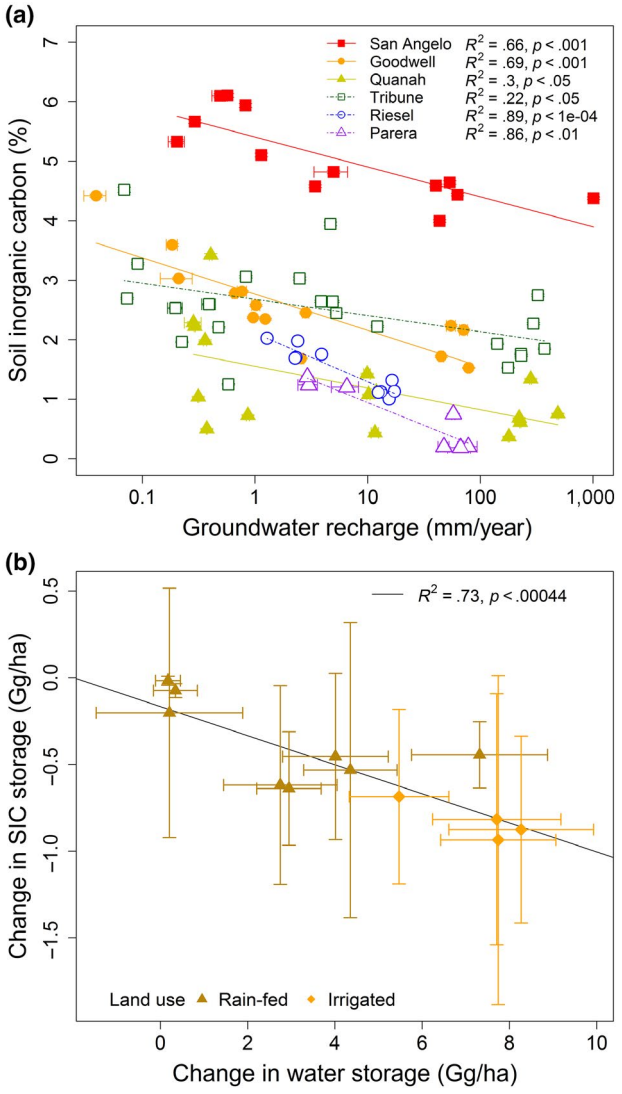

FIGURE 2 (a) Average soil inorganic carbon (SIC) content (%C by weight) to 7.3 m depth by borehole versus estimated groundwater recharge rates from the corresponding boreholes. SIC decreased significantly with higher recharge rates at all sites except at Tribune. Averaging SIC content to 4.9 m depth significantly improves the regression for Goodwell and Tribune, two sites with the most recent conversion to rain-fed cultivation (R^2 of .79 and .41, respectively), indicating that SIC at deeper depths may not have equilibrated with the new recharge rates at these sites. Error bars represent standard error; bars for SIC (*y*-axis) are based on propagation of analytical errors for the weighted averaging (Skoog, Holler, & Crouch, 2017), and bars for recharge rates (*x*-axis) are based on measurements at different depths within a borehole. (b) Change in soil water storage versus change in SIC stock with agricultural conversion of natural vegetation (see also Figure S4). Soil water storage was calculated using gravimetric water content and soil bulk density. All comparisons are to 7.3 m depth except San Angelo (4.9 m), General Levalle (2.4 m), and Rio Bamba (2 m) sites. Error bars represent standard error from replicate cores

SIC increased with depth ($p < .0001$), unlike soil organic carbon storage which typically peaks at the soil surface and decreases with depth. Where we were able to sample to 7.3 m depth for all land uses (Goodwell, Quanah, Tribune, Riesel, Parera), the top 2.4 m of the soil contained less SIC across sites on average, 320 ± 250 Mg C/ha (mean ± *SE*) compared to 460 ± 290 and 830 ± 410 in the second and third 2.4 m of the soil, respectively (Table 2). At the same sites, SIC content also peaked at or below 2 m depth regardless of land use, with half of SIC stored below 4.9 m depth on average (Figure 1). We also observed the largest *changes* in SIC with land-use conversions below 2.4 m, with half of SIC loss occurring below 4.3 m depth on average (Figure 1; Table 2). The deep distribution and large potential for both storage and change in SIC indicate that SIC at even deeper depths may potentially be vulnerable to the downward-advancing wetting front under the cultivated land uses.

Radiocarbon measurements indicate the age and stability of SIC under natural vegetation. All soil profiles under natural vegetation showed low pMC_{SIC} values (<25%; Figure 3) below 1.2 m depth, indicating both that the carbonates likely precipitated and accumulated over tens of thousands of years (prior to the Holocene and likely under a different climate) and that there has been little disturbance to them since their initial precipitation.

In contrast, we observed enhanced equilibration of the old carbonates with modern carbon under croplands compared to native vegetation. pMC_{SIC} under agriculture was higher than under natural vegetation plots, suggesting incorporation of modern carbon into native SIC throughout the >8 m soil profiles within decades of the land-use changes (mixed model $p < .0001$, Table S1, Figure 3). The higher pMC_{SIC} values under agriculture were most evident where larger SIC losses occurred (e.g., 0.5–3 m depths), indicating equilibration of SIC with modern carbon accompanied dissolution of native SIC (Figure 4, first quadrant). The few instances where SIC became less modern (lower pMC_{SIC}) with agricultural conversion were from the top soil layers (<0.5 m), likely from agricultural liming with limestone that has little modern carbon, and from some of the deeper (>3 m) layers where SIC may not yet have equilibrated with modern C (Figure 4, third and fourth quadrants). However, most deeper depths showed increases in pMC_{SIC} under cropland plots, indicating that SIC at these depths could be equilibrating with more modern carbon given enough time under the enhanced recharge. Excluding the limed top soil layers, pMC_{SIC} increased at soil layers where cropland plots gained SIC (second quadrant in Figure 4), suggesting reprecipitation of dissolved SIC in leachates draining from above soil layers with more modern radiocarbon signatures.

$\delta^{13}C$ data for SIC also support equilibration of SIC with more modern carbon sources and point to the crops and dissolved SIC percolating from above soil layers as likely sources of the newly incorporated modern carbon. $\delta^{13}C_{SIC}$ values under cropland moved toward expected $\delta^{13}C$ of carbonate precipitated from crop-respired CO_2, accounting for fractionation during CO_2 dissolution and carbonate precipitation (mixed model $p < .0001$; Table S1, Equation 3; Figure 3). However, in some deeper depths of our sites Tribune and Parera, $\delta^{13}C_{SIC}$ of croplands changed in the opposite direction, reflecting instead the $\delta^{13}C$ of carbonate in shallower layers under natural vegetation and suggesting some equilibration of agricultural SIC with bicarbonate (HCO_3^-) leaching from dissolved SIC of the above soil layers (Figure 3).

TABLE 3 Depth to wetting front and soil inorganic carbonate (SIC) loss front under cultivation

Site	Depth to SIC loss front (m)		Depth to wetting front (m)		Lag (year)[a]
	Rain-fed	Irrigated	Rain-fed	Irrigated	
San Angelo	>4.9[b]	>4.9	>4.9	>4.9	NA, NA
Goodwell	3.7	4.9	5.5	>9.8	38, >6
Quanah	1.2	3.7	5.5	>7.3	26, >1
Tribune	0	7.3	1.2	>9.1	>12, >5
Riesel	7.9	NA	>8.5	NA	>11, NA
Parera	5.5	NA	>9	NA	>4, NA
Gen. Levalle	1.6	NA	>2.5	NA	NA, NA
Rio Bamba	0.2	NA	>2.2	NA	NA, NA

Note: Depth to SIC loss front: the maximum depth (m) of statistically significant SIC loss based on moisture balance (Figure 1; Equation 7), Depth to wetting front: the maximum depth at which statistically significant differences in soil moisture between cropland and natural vegetation plots are observed based on soil moisture content from our replicate cores (for more details, see Section 2.4 and Equation 7 in the methods).

[a]Years since the infiltrating wetting front under cultivated plots drained past the SIC loss front. Average difference in the SIC loss front and wetting front are 2 m for rain-fed and 4 m for irrigated. Average of upper bounds for the lag is ~30 years for carbonate loss to occur after the initial wetting.

[b]The ">" sign indicates that the value is likely underestimated as our sampling depth could not capture the wetting front under some plots.

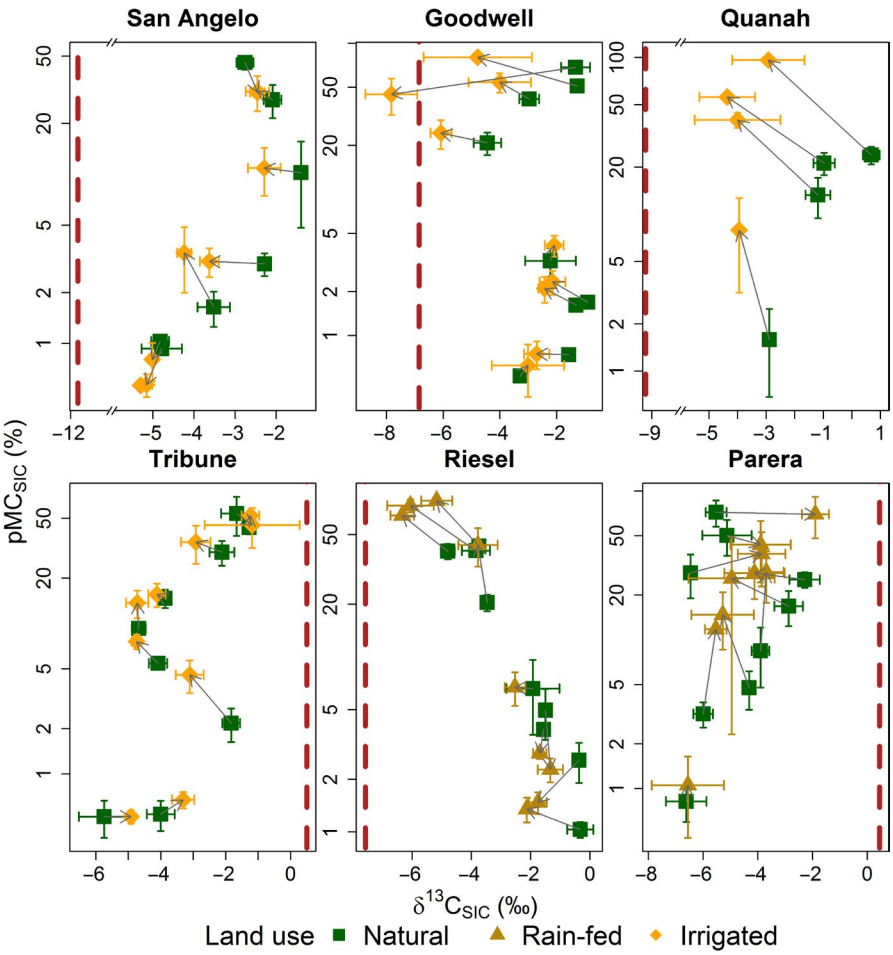

FIGURE 3 Average pMC (percent modern carbon) and $\delta^{13}C$ of soil inorganic carbon (SIC) by land use at each site. pMC decreases with increasing depth. Gray arrows link natural and agricultural plots at corresponding depths. Dotted vertical lines indicate expected $\delta^{13}C$ signature of carbonates precipitated from crop-respired CO_2, estimated from $\delta^{13}C$ of light-fraction soil organic matter (Equation 3). Most depths show increasing pMC with agricultural conversion of natural vegetation, indicating incorporation of modern carbon into SIC ($p < .0001$, Table S1). Most depths also move toward the dotted vertical lines with agricultural conversion, suggesting incorporation of crop-respired carbon into SIC ($p < .0001$, Table S1). However, some notable opposite trends at Tribune and Parera sites also suggest some of the new precipitates under cultivation may be from bicarbonate of dissolved SIC leaching from above layers

In our mixed model, bicarbonate-C in soil water extracts was lower on average by 3.9 and 5.7 mg C/kg soil in rain-fed and irrigated cropland plots, respectively, compared to their paired natural vegetation plots, indicating that agricultural acidification may also have contributed to SIC loss by reducing the buffer capacity of the soils and degassing of the carbonates (Table 2; Table S1; mixed model

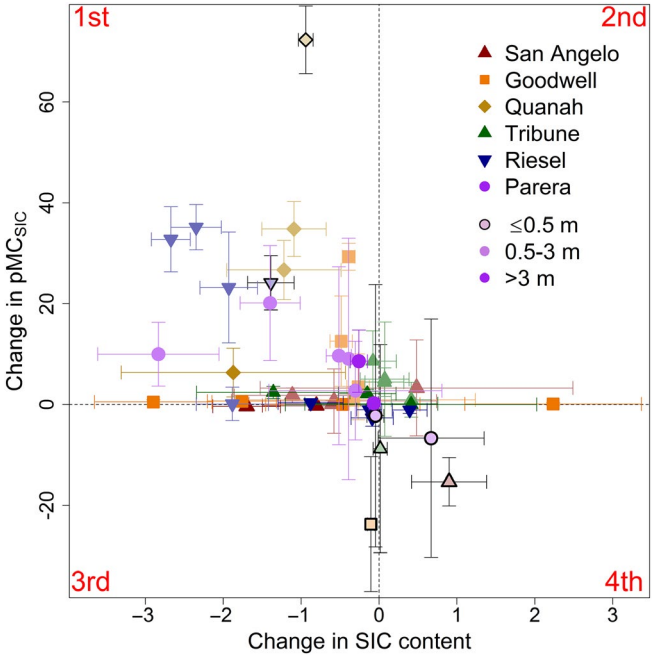

FIGURE 4 Changes in soil inorganic carbon (SIC) content and pMC of SIC at each site. Demarcating four quadrants, a vertical dotted line denotes no changes in SIC content, and a horizontal dotted line denotes no changes in pMC of SIC. The shallowest samples (≤0.5 m deep; symbols with black outlines) tend to decrease in pMC (mostly in third and fourth quadrants), reflecting incorporation of ancient carbon from limestones used in agricultural liming. Excluding the shallowest samples, loss of SIC results in increases in pMC (first quadrant), supporting the hypothesis that dissolution of SIC leads to equilibration with more modern carbon. SIC gain also results in increases in pMC (second quadrant), indicating SIC precipitation may involve bicarbonate ions of more modern origins, either atmospheric or in leachates of dissolved SIC from above soil layers. Error bars represent standard errors from replicate cores, calculated using propagation of errors (Skoog et al., 2017)

$p < .0007$ and .0001 for rain-fed and irrigated plots, respectively). Significantly lower bicarbonate concentrations were observed for the entire sampled profile at some cropland plots, suggesting agricultural soil acidification at these sites may have permeated through >8 m depth (Figure S5; Goodwell and Quanah sites).

4 | DISCUSSION

Our results point to a potentially dynamic soil carbonate pool that is sensitive to contemporary changes in vegetation and hydrology. The incorporation of modern carbon of crop origin into SIC stocks under croplands (Figure 3) suggests that the SIC, which likely has equilibrated little in the last tens of thousands of years with modern carbon (as evidenced by low pMC_{SIC} values >2 m depth), can adjust rapidly with decades-old land-use changes. Moisture balance further indicated a ~30-year lag between the onset of enhanced recharge and observable SIC losses (Equation 7; Table 3). If the dissolved carbonates (DIC) do not reprecipitate during transport along the soil-, ground-, and surface-water flow path, our results would add to the growing body of evidence that SIC may interact with atmospheric CO_2 in decadal timescales, as discussed in more detail below.

Our data suggest a strong coupling between the SIC cycle and hydrology as mediated by the vegetation. Greater deep drainage with agricultural conversion (often by three orders of magnitude; Figure 2) may represent a sudden pedogenic forcing that elicits a rapid response (Chadwick & Chorover, 2001; Chen, Zhang, & Effland, 2011). Decreasing SIC with increasing soil moisture and deep drainage, both between land uses and across our sites along the humidity gradient, suggests greater leaching of weathered products under wetter conditions (Figure 2; Figure S6). Greater loss of SIC with irrigation relative to rain-fed cultivation further highlights the influence of water, rather than differences in land-use management such as tillage or fertilization, on SIC losses. In addition to being a medium for dissolution and transport, greater water content may allow SIC to quickly re-equilibrate with pore space CO_2 (Amundson et al., 1994; Gocke et al., 2010; Van Breemen & Protz, 1988), as indicated by more modern C signatures with increasing humidity in our mixed model analysis (i.e., increasing PWE; Table S1). Carbonate chemistry in variably saturated media, such as the vadose zone we sampled, is sensitive to the hydrologically accessible reactive surface area (Xu, Sonnenthal, Spycher, & Pruess, 2006). Relative to the previously dry and inert soil matrix under natural vegetation, increased reactive area of dampened finer laminar coating of disseminated carbonates under croplands may be responsible for the greater SIC dissolution (Stumm & Wollast, 1990; Zamanian et al., 2016).

Deep distributions of both SIC storage *and* losses from agricultural acceleration of weathering (50% below 4.9 and 4.3 m on average, respectively) highlight the vulnerability of the large SIC stocks held in the deeper soil to land surface changes, in our case the downward-advancing wetting front generated under cultivated land uses (Marion, Schlesinger, & Fonteyn, 1985). We expect SIC losses to continue as these wetting fronts infiltrate deeper horizons where larger SIC stocks are held (Table 3). The SIC losses were also more than an order of magnitude larger than the changes at the same sites in the organic carbon stocks (462 vs. 29 Mg C/ha on average), a pool often considered for carbon sequestration in climate change mitigation strategies, and larger even than biomass in some of the most carbon-dense ecosystems in the world (~400 Mg C/ha, Table 2; Keith, Mackey, & Lindenmayer, 2009). To further highlight the importance of depth, our conclusions would be drastically different (e.g., only half of cropland plots would show SIC losses) if we limited our sampling depth to the median of those in our literature review database (0.75 m, Appendix S1), where we indeed observed general increasing trend in SIC with crop cultivation (Table S2). The deep distribution and losses of SIC highlight importance of deeper sampling for a more complete understanding of terrestrial carbon dynamics and its missing sinks (Ballantyne, Alden, Miller, Tans, & White, 2012; Jackson et al., 2002; Liu, Dreybrodt, & Wang, 2010).

The final fate of lost SIC cannot be assessed with our observations, yet its understanding is critical in determining whether

the SIC mobilization represents a net ecosystem carbon source or sink. Three possible pathways for the lost SIC are degassing, leaching, or reprecipitation (Equation 1), requiring different chemical and hydrological conditions and having different consequences on net CO_2 emissions. The amount and type of fertilizer used likely determine the extent of the degassing pathway (i.e., carbon source). The upper bounds for CO_2 emission from the SIC pool are 0.36–2.8 Mg C ha^{-1} $year^{-1}$, drawing from agricultural acidification rates of 30–240 kmol H^+ ha^{-1} $year^{-1}$ from use of nitrogen fertilizers (Guo et al., 2010). Estimates taking into account incomplete acid reactions with bicarbonate are lower, with a range of 0.005–0.3 Mg C ha^{-1} $year^{-1}$ for Australia (Ahmad, Singh, Dalal, & Dijkstra, 2015) and a global estimate of ~0.074 Mg C ha^{-1} $year^{-1}$ (Zamanian, Zarebanadkouki, & Kuzyakov, 2018). The soil acidification under cropland plots throughout our sampling depth indicates some degassing may have occurred at our sites (Table 2; Figure S5). We also note that greater fluxes of water and strong acids such as nitric acid from agricultural activities may increase CO_2 consumption via silicate weathering, but this may be offset by increased CO_2 degassing (Guo, Wang, Vogt, Zhang, & Liu, 2015; Pacheco, Landim, & Szocs, 2013; West, Galy, & Bickle, 2005).

The fate of the carbon (i.e., DIC) mobilized by the leaching pathway and its impact on the carbon cycle hinge on the hydrologic conditions and connectivity of the soil-, ground-, and surface waters. Barnes and Raymond (2009) found ~4 times greater export of DIC from agricultural watersheds compared to forested ones. ^{14}C analyses revealed that DIC in ground- and river-water in agricultural watersheds was also older than that of natural vegetation, supporting its SIC origins (Grimm, Spero, Harding, & Guilderson, 2017; Li, Wang, Houghton, & Tang, 2015). As carbonate dissolution can consume CO_2 (Equation 1), the leached DIC entering groundwaters with long residence times may be sequestered long-term (i.e., carbon sink). Bicarbonate leaching to ground water could account for up to 0.067 Mg C ha^{-1} $year^{-1}$ using bicarbonate concentrations below the root zone in soil water extracts and recharge rates from our field data (Table 2), which is much lower than the range of 0.14–3.6 Mg C ha^{-1} $year^{-1}$ from other studies (Bughio et al., 2015; Kalbitz et al., 2013; Monger et al., 2015; Yu et al., 2014). In contrast, rapid connections to surface waters may create more uncertainty in the fate of the mobilized carbon, as DIC in surface waters may be exposed to conditions more conducive to degassing during transport to the ocean, where the composition of the mixing seawater will ultimately affect further carbonate reactions or uptake and sequestration by the biota (e.g., Berner, Westrich, Graber, Smith, & Martens, 1978; Liu & Dreybrodt, 2014; Liu et al., 2010; Mucci, 1986).

The estimates of the two pathways discussed above are modest relative to SIC losses we observed, implying either reprecipitation of dissolved SIC past our sampling depth (no net carbon flux), storage of bicarbonate in slow-moving aquifers, or greater interactive effects of agricultural practices on SIC (Ahmad et al., 2015; Dong, Duan, Wang, & Hu, 2016). $\delta^{13}C_{SIC}$ data support some reprecipitation of SIC with crop-respired CO_2 and/or DIC leaching from the above layers; however, given the loss of alkalinity under croplands despite regular liming (Table 2; Figure S5), the extent of this pathway may also be limited (Figure 3).

Though we could not assess the fate of the accelerated weathering of carbonates, dissolution of solid-phase SIC to more reactive mobile ions would likely increase exposure to different environmental conditions during transport and probability of further transformations. In the context of enhanced weathering as a means to achieve negative emissions (Fuss et al., 2018; Lawrence et al., 2018), our evidence for a sensitive SIC pool reacting to hydrological changes, along with the quantity, rate, and extent of the SIC losses, highlights the need for further evaluation of net sink or source potential of the SIC pool (i.e., fate of DIC) and associated time lags under changing land uses.

ACKNOWLEDGEMENTS

This work was supported by the National Science Foundation (DEB #0717191, IOS #0920355, GRFP #2006044266, DDIG #0910294) and European Commission (Marie Curie: ELSIC FP7-PEOPLE-2013-IEF-626334). We wish to thank Nancy Scott and Virginia Palacios for their assistance with the database, Eugenia Beget for providing access to weather data from Argentina, and the Jackson lab, Bernhardt lab, Grupo Estudios Ambientales, and Max Planck Institute for Biogeochemistry for their help in the laboratory and the field, and the Richter Soils lab for the use of the Geoprobe. We also thank many landowners and personnel at the following research centers who provided access to the sites and logistical support: Grupo Estudios Ambientales in San Luis, Argentina, Western Kansas Agricultural Research Center in Tribune, Oklahoma Panhandle research and extension center in Goodwell, Texas AgriLife Research and Extension Centers at Vernon and San Angelo, and USDA-ARS Grassland Soil and Water Research Laboratory in Temple, TX.

DATA AVAILABILITY STATEMENT

Data supporting our analysis can be found in the PANGAEA data repository (https://pangaea.de).

ORCID

John H. Kim https://orcid.org/0000-0002-7845-5692

REFERENCES

Ahmad, W., Singh, B., Dalal, R. C., & Dijkstra, F. A. (2015). Carbon dynamics from carbonate dissolution in Australian agricultural soils. *Soil Research*, *53*(2), 144–153. https://doi.org/10.1071/SR14060

Allen, R. G., Pereira, L. S., Raes, D., & Smith, M. (1998). *Crop evapotranspiration. Guidelines for computing crop water requirements*. FAO Irrigation and drainage, paper 56. Rome, Italy: Food and Agriculture Organizatoin of the United Nations.

Allison, G. B., & Hughes, M. W. (1983). The use of natural tracers as indicators of soil-water movement in a temperate semi-arid region. *Journal of Hydrology*, *60*(1–4), 157–173. https://doi.org/10.1016/0022-1694(83)90019-7

American Public Health Association (APHA), American Water Works Association (AWWA), & Water Pollution Control Federation (WPCF). (1992). *Standard methods for the examination of water and wastewater* (18th ed.). Washington, DC: APHA.

Amundson, R., Wang, Y., Chadwick, O., Trumbore, S., McFadden, L., McDonald, E., … DeNiro, M. (1994). Factors and processes governing the ^{14}C content of carbonate in desert soils. *Earth and Planetary Science Letters*, *125*(1), 385–405. https://doi.org/10.1016/0012-821X(94)90228-3

An, H., Wu, X., Zhang, Y., & Tang, Z. (2019). Effects of land-use change on soil inorganic carbon: A meta-analysis. *Geoderma*, *353*, 273–282. https://doi.org/10.1016/j.geoderma.2019.07.008

Arkley, R. J. (1963). Calculation of carbonate and water movement in soil from climatic data. *Soil Science*, *96*(4), 239–248. https://doi.org/10.1097/00010694-196310000-00003

Assayag, N., Rivé, K., Ader, M., Jézéquel, D., & Agrinier, P. (2006). Improved method for isotopic and quantitative analysis of dissolved inorganic carbon in natural water samples. *Rapid Communications in Mass Spectrometry*, *20*(15), 2243–2251. https://doi.org/10.1002/rcm.2585

Ballantyne, A., Alden, C., Miller, J., Tans, P., & White, J. (2012). Increase in observed net carbon dioxide uptake by land and oceans during the past 50 years. *Nature*, *488*(7409), 70–72. https://doi.org/10.1038/nature11299

Barnes, R. T., & Raymond, P. A. (2009). The contribution of agricultural and urban activities to inorganic carbon fluxes within temperate watersheds. *Chemical Geology*, *266*(3–4), 318–327. https://doi.org/10.1016/j.chemgeo.2009.06.018

Benjamini, Y., & Hochberg, Y. (1995). Controlling the false discovery rate: A practical and powerful approach to multiple testing. *Journal of the Royal Statistical Society: Series B (Methodological)*, *57*(1), 289–300.

Berhongaray, G., Alvarez, R., De Paepe, J., Caride, C., & Cantet, R. (2013). Land use effects on soil carbon in the Argentine Pampas. *Geoderma*, *192*, 97–110. https://doi.org/10.1016/j.geoderma.2012.07.016

Berner, R. A. (2003). The long-term carbon cycle, fossil fuels and atmospheric composition. *Nature*, *426*(6964), 323–326.

Berner, R. A., Lasaga, A. C., & Garrels, R. (1983). The carbonate-silicate geochemical cycle and its effect on atmospheric carbon dioxide over the past 100 million years. *American Journal of Science*, *283*(7), 641–683. https://doi.org/10.2475/ajs.283.7.641

Berner, R. A., Westrich, J. T., Graber, R., Smith, J., & Martens, C. S. (1978). Inhibition of aragonite precipitation from supersaturated seawater; a laboratory and field study. *American Journal of Science*, *278*(6), 816–837. https://doi.org/10.2475/ajs.278.6.816

Birkeland, P. W. (1999). *Soils and geomophology*. New York: Oxford University Press.

Bughio, M. A., Wang, P., Meng, F., Qing, C., Kuzyakov, Y., Wang, X., & Junejo, S. (2015). Neoformation of pedogenic carbonates by irrigation and fertilization and their contribution to carbon sequestration in soil. *Geoderma*, *262*, 12–19. https://doi.org/10.1016/j.geoderma.2015.08.003

Cerling, T. E., Quade, J., Wang, Y., & Bowman, J. (1989). Carbon isotopes in soils and palaeosols as ecology and palaeoecology indicators. *Nature*, *341*(6238), 138–139.

Chadwick, O. A., & Chorover, J. (2001). The chemistry of pedogenic thresholds. *Geoderma*, *100*(3–4), 321–353. https://doi.org/10.1016/S0016-7061(01)00027-1

Chen, L.-M., Zhang, G.-L., & Effland, W. R. (2011). Soil characteristic response times and pedogenic thresholds during the 1000-year evolution of a paddy soil chronosequence. *Soil Science Society of America Journal*, *75*(5), 1807–1820. https://doi.org/10.2136/sssaj2011.0006

Chichester, F. W., & Chaison, R. F. (1992). Analysis of carbon in calcareous soils using a two temperature dry combustion infrared instrumental procedure. *Soil Science*, *153*(3), 237–241. https://doi.org/10.1097/00010694-199203000-00007

Dong, W., Duan, Y., Wang, Y., & Hu, C. (2016). Reassessing carbon sequestration in the North China Plain via addition of nitrogen. *Science of the Total Environment*, *563*, 138–144. https://doi.org/10.1016/j.scitotenv.2016.04.115

Fuss, S., Lamb, W. F., Callaghan, M. W., Hilaire, J., Creutzig, F., Amann, T., … Minx, J. C. (2018). Negative emissions—Part 2: Costs, potentials and side effects. *Environmental Research Letters*, *13*(6), 063002. https://doi.org/10.1088/1748-9326/aabf9f

Gao, P., Xu, X., Zhou, L., Pack, M. A., Griffin, S., Santos, G. M., … Liu, K. (2014). Rapid sample preparation of dissolved inorganic carbon in natural waters using a headspace-extraction approach for radiocarbon analysis by accelerator mass spectrometry. *Limnology and Oceanography: Methods*, *12*(4), 174–190.

Gocke, M., Pustovoytov, K., & Kuzyakov, Y. (2010). Effect of CO_2 concentration on the initial recrystallization rate of pedogenic carbonate — Revealed by ^{14}C and ^{13}C labeling. *Geoderma*, *155*(3–4), 351–358. https://doi.org/10.1016/j.geoderma.2009.12.018

Goddéris, Y., & Brantley, S. L. (2013). Earthcasting the future critical zone. *Elementa: Science of the Anthropocene*, *1*(1), 000019. https://doi.org/10.12952/journal.elementa.000019

Grimm, B. L., Spero, H. J., Harding, J. M., & Guilderson, T. P. (2017). Seasonal radiocarbon reservoir ages for the 17th century James River, Virginia estuary. *Quaternary Geochronology*, *41*, 119–133. https://doi.org/10.1016/j.quageo.2017.03.002

Guo, J., Liu, X., Zhang, Y., Shen, J., Han, W., Zhang, W., … Zhang, F. (2010). Significant acidification in major Chinese croplands. *Science*, *327*(5968), 1008–1010.

Guo, J., Wang, F., Vogt, R. D., Zhang, Y., & Liu, C.-Q. (2015). Anthropogenically enhanced chemical weathering and carbon evasion in the Yangtze Basin. *Scientific Reports*, *5*(1), 1–8. https://doi.org/10.1038/srep11941

Instituto Nacional de Tecnología Agropecuaria (INTA). (2010). *Agrometeorologia*. Retrieved from http://www.inta.gov.ar/index.asp

Intergovernmental Panel on Climate Change (IPCC). (2014). Mitigation of climate change. *Contribution of Working Group III to the Fifth Assessment Report of the Intergovernmental Panel on Climate Change*, *1454*.

Jackson, R. B., Banner, J. L., Jobbágy, E. G., Pockman, W. T., & Wall, D. H. (2002). Ecosystem carbon loss with woody plant invasion of grasslands. *Nature*, *418*(6898), 623–626.

Jenny, H., & Leonard, C. D. (1934). Functional relationships between soil properties and rainfall. *Soil Science*, *38*(5), 363–382. https://doi.org/10.1097/00010694-193411000-00004

Jobbágy, E. G., & Jackson, R. B. (2000). The vertical distribution of soil organic carbon and its relation to climate and vegetation. *Ecological Applications*, *10*(2), 423–436. https://doi.org/10.1890/1051-0761(2000)010[0423:TVDOSO]2.0.CO;2

Kalbitz, K., Kaiser, K., Fiedler, S., Kölbl, A., Amelung, W., Bräuer, T., … Jahn, R. (2013). The carbon count of 2000 years of rice cultivation. *Global Change Biology*, *19*(4), 1107–1113.

Keith, H., Mackey, B. G., & Lindenmayer, D. B. (2009). Re-evaluation of forest biomass carbon stocks and lessons from the world's most carbon-dense forests. *Proceedings of the National Academy of Sciences of the United States of America*, *106*(28), 11635–11640. https://doi.org/10.1073/pnas.0901970106

Kelly, E. F., Amundson, R. G., Marino, B. D., & DeNiro, M. J. (1991). Stable carbon isotopic composition of carbonate in Holocene grassland soils. *Soil Science Society of America Journal*. https://doi.org/10.2136/sssaj1991.03615995005500060025x

Kim, J. H., & Jackson, R. B. (2012). A global analysis of groundwater recharge for vegetation, climate, and soils. *Vadose Zone Journal*, *11*(1). https://doi.org/10.2136/vzj2011.0021RA

Kim, J. H., Jobbágy, E. G., & Jackson, R. B. (2016). Trade-offs in water and carbon ecosystem services with land-use changes in grasslands. *Ecological Applications*, *26*(8), 1633–1644. https://doi.org/10.1890/15-0863.1

Klute, A. (1986). *Methods of soil analysis. Part 1, Physical and mineralogical methods*. Madison, WI: Soil Science Society of America.

Kuzyakov, Y., & Zamanian, K. (2019). Reviews and syntheses: Agropedogenesis-humankind as the sixth soil-forming factor and attractors of agricultural soil degradation. *Biogeosciences*, *16*(24), 4783–4803. https://doi.org/10.5194/bg-16-4783-2019

Lal, R., & Kimble, J. M. (2000). Pedogenic carbonates and the global carbon cycle. In R. Lal, J. M. Kimble, H. Eswaran, & B. A. Stewart (Eds.), *Global climate change and pedogenic carbonates* (pp. 1–13). Boca Raton, FL: Lewis.

Landi, A., Mermut, A., & Anderson, D. (2003). Origin and rate of pedogenic carbonate accumulation in Saskatchewan soils, Canada. *Geoderma*, *117*(1–2), 143–156. https://doi.org/10.1016/S0016-7061(03)00161-7

Lawrence, M. G., Schäfer, S., Muri, H., Scott, V., Oschlies, A., Vaughan, N. E., … Scheffran, J. (2018). Evaluating climate geoengineering proposals in the context of the Paris Agreement temperature goals. *Nature Communications*, *9*(1), 1–19. https://doi.org/10.1038/s41467-018-05938-3

Li, D., & Shao, M. (2015). Temporal stability of soil water storage in three landscapes in the middle reaches of the Heihe River, northwestern China. *Environmental Earth Sciences*, *73*(7), 3095–3107. https://doi.org/10.1007/s12665-014-3604-z

Li, Y., Wang, Y. G., Houghton, R., & Tang, L. S. (2015). Hidden carbon sink beneath desert. *Geophysical Research Letters*, *42*(14), 5880–5887. https://doi.org/10.1002/2015GL064222

Liu, R., Li, Y., & Wang, Q. X. (2011). Variations in water and CO_2 fluxes over a saline desert in western China. *Hydrological Processes*, *26*, 513–522. https://doi.org/10.1002/hyp.8147

Liu, Z., & Dreybrodt, W. (2014). Significance of the carbon sink produced by H_2O–carbonate–CO_2–aquatic phototroph interaction on land. *Science Bulletin*, *60*(2), 1–10.

Liu, Z., Dreybrodt, W., & Wang, H. (2010). A new direction in effective accounting for the atmospheric CO_2 budget: Considering the combined action of carbonate dissolution, the global water cycle and photosynthetic uptake of DIC by aquatic organisms. *Earth-Science Reviews*, *99*(3–4), 162–172. https://doi.org/10.1016/j.earscirev.2010.03.001

Magaritz, M., & Amiel, A. J. (1981). Influence of intensive cultivation and irrigation on soil properties in the Jordan Valley, Israel: Recrystallization of carbonate minerals. *Soil Science Society of America Journal*, *45*(6), 1201–1205. https://doi.org/10.2136/sssaj1981.03615995004500060038x

Marion, G. M., Schlesinger, W., & Fonteyn, P. (1985). CALDEP: A regional model for soil $CaCO_3$ (caliche) deposition in southwestern deserts. *Soil Science*, *139*(5), 468. https://doi.org/10.1097/00010694-198505000-00014

Monger, H. C., Kraimer, R. A., Khresat, S., Cole, D. R., Wang, X., & Wang, J. (2015). Sequestration of inorganic carbon in soil and groundwater. *Geology*, *43*(5), 375–378. https://doi.org/10.1130/G36449.1

Moody, P., & Aitken, R. (1997). Soil acidification under some tropical agricultural systems. 1. Rates of acidification and contributing factors. *Australian Journal of Soil Research*, *35*(1), 163–173.

Mucci, A. (1986). Growth kinetics and composition of magnesian calcite overgrowths precipitated from seawater: Quantitative influence of orthophosphate ions. *Geochimica et Cosmochimica Acta*, *50*(10), 2255–2265. https://doi.org/10.1016/0016-7037(86)90080-3

National Oceanic and Atmospheric Administration (NOAA), National Climatic Data Center. (2011). NOAA National Centers for Environmental Information. Retrieved from https://www.ncdc.noaa.gov/cdo-web/

New, M., Lister, D., Hulme, M., & Makin, I. (2002). A high-resolution data set of surface climate over global land areas. *Climate Research*, *21*(1), 1–25. https://doi.org/10.3354/cr021001

Pacheco, F. A., Landim, P. M., & Szocs, T. (2013). Anthropogenic impacts on mineral weathering: A statistical perspective. *Applied Geochemistry*, *36*, 34–48. https://doi.org/10.1016/j.apgeochem.2013.06.012

Papiernik, S., Lindstrom, M., Schumacher, T., Schumacher, J., Malo, D., & Lobb, D. (2007). Characterization of soil profiles in a landscape affected by long-term tillage. *Soil and Tillage Research*, *93*(2), 335–345. https://doi.org/10.1016/j.still.2006.05.007

Phillips, F. M. (1994). Environmental tracers for water-movement in desert soils of the American Southwest. *Soil Science Society of America Journal*, *58*(1), 15–24. https://doi.org/10.2136/sssaj1994.03615995005800010003x

Ramankutty, N., Evan, A. T., Monfreda, C., & Foley, J. A. (2008). Farming the planet: 1. Geographic distribution of global agricultural lands in the year 2000. *Global Biogeochemical Cycles*, *22*, GB1003.

Richter Jr., D. D. (2007). Humanity's transformation of Earth's soil: Pedology's new frontier. *Soil Science*, *172*(12), 957–967. https://doi.org/10.1097/ss.0b013e3181586bb7

Scanlon, B. R., Reedy, R. C., Stonestrom, D. A., Prudic, D. E., & Dennehy, K. F. (2005). Impact of land use and land cover change on groundwater recharge and quality in the southwestern US. *Global Change Biology*, *11*(10), 1577–1593. https://doi.org/10.1111/j.1365-2486.2005.01026.x

Schimel, D. S., Enting, I. G., Heimann, M., Wigley, T. M. L., Raynaud, D., Alves, D., & Siegenthaler, U. (1995). CO_2 and the carbon cycle. In J. T. Houghton, L. G. M. Filho, J. P. Bruce, H. Lee, B. A. Callander, & E. F. Haites (Eds.), *Climate change 1994: Radiative forcing of climate change and evaluation of the IPCC IS92 emission scenarios* (pp. 7–34). Cambridge, UK: Cambridge University Press.

Schlesinger, W. H. (1982). Carbon storage in the caliche of arid soils: A case study from Arizona. *Soil Science*, *133*(4), 247. https://doi.org/10.1097/00010694-198204000-00008

Schlesinger, W. H. (2017). An evaluation of abiotic carbon sinks in deserts. *Global Change Biology*, *23*(1), 25–27. https://doi.org/10.1111/gcb.13336

Skoog, D. A., Holler, F. J., & Crouch, S. R. (2017). *Principles of instrumental analysis*. Boston, MA: Cengage Learning.

Sohi, S. P., Mahieu, N., Arah, J. R., Powlson, D. S., Madari, B., & Gaunt, J. L. (2001). A procedure for isolating soil organic matter fractions suitable for modeling. *Soil Science Society of America Journal*, *65*(4), 1121–1128. https://doi.org/10.2136/sssaj2001.6541121x

St. Arnaud, R. J. (1979). Nature and distribution of secondary soil carbonates within landscapes in relation to soluble Mg^{++}/Ca^{++} ratios. *Canadian Journal of Soil Science*, *59*, 87–98. https://doi.org/10.4141/cjss79-009

Steinhof, A. (2013). Data analysis at the Jena ^{14}C laboratory. *Radiocarbon*, *55*(2), 282–293. https://doi.org/10.1017/S0033822200057386

Steinhof, A. (2014). Analysis of the background of the Jena ^{14}C-AMS facility. *Nuclear Instruments and Methods in Physics Research Section B: Beam Interactions with Materials and Atoms*, *331*, 238–242. https://doi.org/10.1016/j.nimb.2013.12.038

Steinhof, A., Altenburg, M., & Machts, H. (2017). Sample preparation at the Jena ^{14}C laboratory. *Radiocarbon*, *59*(3), 815–830. https://doi.org/10.1017/RDC.2017.50

Stumm, W., & Wollast, R. (1990). Coordination chemistry of weathering: Kinetics of the surface-controlled dissolution of oxide minerals. *Reviews of Geophysics*, *28*(1), 53–69. https://doi.org/10.1029/RG028i001p00053

Tamir, G., Shenker, M., Heller, H., Bloom, P. R., Fine, P., & Bar-Tal, A. (2011). Can soil carbonate dissolution lead to overestimation of soil respiration? *Soil Science Society of America Journal*, *75*(4), 1414–1422. https://doi.org/10.2136/sssaj2010.0396

United States Department of Agriculture (USDA) Soil Survey Staff. (2009). Web soil survey. Natural Resources Conservation Service, Soil Survey Staff. Retrieved from http://websoilsurvey.nrcs.usda.gov/

Van Breemen, N., & Protz, R. (1988). Rates of calcium carbonate removal from soils. *Canadian Journal of Soil Science*, *68*(2), 449–454. https://doi.org/10.4141/cjss88-042

Walker, G. R., Jolly, I. D., & Cook, P. G. (1991). A new chloride leaching approach to the estimation of diffuse recharge following a change in land-use. *Journal of Hydrology*, *128*(1–4), 49–67. https://doi.org/10.1016/0022-1694(91)90131-Z

Wang, Z., Liu, B., & Zhang, Y. (2009). Soil moisture of different vegetation types on the Loess Plateau. *Journal of Geographical Sciences*, *19*(6), 707. https://doi.org/10.1007/s11442-009-0707-7

West, A. J., Galy, A., & Bickle, M. (2005). Tectonic and climatic controls on silicate weathering. *Earth and Planetary Science Letters*, *235*(1–2), 211–228. https://doi.org/10.1016/j.epsl.2005.03.020

Williams, E. L., Walter, L. M., Ku, T. C. W., Kling, G. W., & Zak, D. R. (2003). Effects of CO_2 and nutrient availability on mineral weathering in controlled tree growth experiments. *Global Biogeochemical Cycles*, *17*(2), 1041. https://doi.org/10.1029/2002GB001925

Wu, H., Guo, Z., Gao, Q., & Peng, C. (2009). Distribution of soil inorganic carbon storage and its changes due to agricultural land use activity in China. *Agriculture, Ecosystems & Environment*, *129*(4), 413–421. https://doi.org/10.1016/j.agee.2008.10.020

Xu, T., Sonnenthal, E., Spycher, N., & Pruess, K. (2006). TOUGHREACT—A simulation program for non-isothermal multiphase reactive geochemical transport in variably saturated geologic media: Applications to geothermal injectivity and CO_2 geological sequestration. *Computers & Geosciences*, *32*(2), 145–165. https://doi.org/10.1016/j.cageo.2005.06.014

Yu, P., Li, Q., Jia, H., Li, G., Zheng, W., Shen, X., … Zhou, D. (2014). Effect of cultivation on dynamics of organic and inorganic carbon stocks in Songnen plain. *Agronomy Journal*, *106*(5), 1574–1582. https://doi.org/10.2134/agronj14.0113

Zamanian, K., Pustovoytov, K., & Kuzyakov, Y. (2016). Pedogenic carbonates: Forms and formation processes. *Earth-Science Reviews*, *157*, 1–17. https://doi.org/10.1016/j.earscirev.2016.03.003

Zamanian, K., Zarebanadkouki, M., & Kuzyakov, Y. (2018). Nitrogen fertilization raises CO_2 efflux from inorganic carbon: A global assessment. *Global Change Biology*, *24*(7), 2810–2817.

Zárate, M. A., & Tripaldi, A. (2012). The aeolian system of central Argentina. *Aeolian Research*, *3*(4), 401–417. https://doi.org/10.1016/j.aeolia.2011.08.002

SUPPORTING INFORMATION

Additional supporting information may be found online in the Supporting Information section.

How to cite this article: Kim JH, Jobbágy EG, Richter DD, Trumbore SE, Jackson RB. Agricultural acceleration of soil carbonate weathering. *Glob Change Biol*. 2020;26:5988–6002. https://doi.org/10.1111/gcb.15207